Electron spin resonance in antiferro-quadrupolar-ordered CeB_6

P. Schlottmann
Department of Physics, Florida State University, Tallahassee, Florida 32306, USA
(Received 17 May 2012; revised manuscript received 19 July 2012; published 21 August 2012)

CeB_6 is a *cubic* heavy-fermion compound with a Γ_8 ground quartet for which an ESR signal was observed. All other Ce or Yb compounds displaying an ESR signal have strong magnetic anisotropy and ferromagnetic correlations among the spins. The role of the ferromagnetic correlations is to narrow the resonance width rendering the signal observable. In CeB_6 the orbital content of the Γ_8 quartet gives rise to an antiferro-quadrupolar-ordered phase below 4 K. Single ions with a Γ_8 ground multiplet are expected to display four transitions, however, only one has been observed. The following questions are addressed in this paper: (1) why is only one transition seen, (2) why is this transition observed if the Kondo temperature is comparable to the linewidth and the resonance frequency, and (3) are there ferromagnetic correlations between the Ce ions? The answer to these questions is associated with the antiferro-quadrupolar order. While for other Ce and Yb compounds with ESR signal it is difficult to distinguish if the resonance is due to localized spins or conducting heavy electron spins, an itinerant picture within the antiferro-quadrupolar phase is necessary for CeB_6.

DOI: 10.1103/PhysRevB.86.075135 PACS number(s): 71.27.+a, 72.15.Qm, 75.20.Hr, 76.30.−v

I. INTRODUCTION

There is an intimate relation between the relaxation rate for a Kondo impurity and the Kondo susceptibility, $\chi_0/T_1 \approx$ constant for all T.[1] At $\omega = T = H = 0$, this relation is exact (for $S = 1/2$ the constant is $2/\pi$) and known as the Shiba relation.[2] This result suggests that an electron spin resonance (ESR) signal could not be observed in heavy-fermion compounds due to the broad linewidth proportional to the Kondo temperature. This common belief was recently proven wrong, when an ESR signal was found in single crystals of the quantum critical system $YbRh_2Si_2$,[3] and since then in several other Yb compounds, e.g., $YbIr_2Si_2$,[4] YbRh,[5] and $YbCo_2Zn_{20}$,[6] and one Ce compound CeRuPO.[7] The resonance was attributed to the Yb^{3+} and Ce^{3+} ions despite of their rather large Kondo temperature. All of the above compounds are very anisotropic and have ferromagnetic correlations among the rare-earth spins.[5] The resonance in $YbRh_2Si_2$ has been confirmed by other groups[8,9] and on a different batch of samples[9] as well as followed up to 360 GHz.[10]

The observed resonances have a Dysonian line shape,[11] as expected from the skin depth and spin diffusion in a metallic environment. ESR of magnetic ions in a metal[12] as well as the resonance of conduction electrons[11] have a similar Dysonian line shape. The analysis of the data performed within the known framework of ESR of magnetic impurities in metals,[12] i.e., single ions with localized spins resonating independently, is consistent with the g-factor anisotropy expected for Yb^{3+} ions in a tetragonal crystalline electric field as well as with the linewidth. It has been estimated that in $YbRh_2Si_2$ more than 60% of the Yb^{3+} ions contribute to the ESR signal.[13] On the other hand, in the case of conducting heavy fermions, the g shift is dominated by the one of the f electrons and is going to have the crystalline field anisotropies of the rare-earth sites. It is hard to justify an intensity corresponding to more than 60% of the Yb ions, since a resonance of conduction electrons takes place only close to the Fermi level. Based solely on ESR it is then difficult, if not impossible, to decide, if the resonances arise from localized moments or the carriers in a heavy-electron band.[14]

Recently, Abrahams and Wölfle[15] studied the linewidth of the ESR signal for a heavy-fermion compound within the framework of the Anderson lattice. They obtained that the heavy mass in conjunction with ferromagnetic fluctuations can lead to observable narrow resonances. The heavy mass is equivalent with arguing with a small Kondo temperature for the lattice, but is not enough to produce an observable ESR signal. The ferromagnetic correlations further reduce the linewidth of the signal. Wölfle and Abrahams[16] have applied their theory to the Fermi liquid regime for $YbRh_2Si_2$ and found excellent agreement with the experimental data. They also extended the description to the non-Fermi liquid regime of this material and found a close relation of the T dependence of the specific heat and spin susceptibility with the observed T dependence of the g shift and the linewidth.

Schlottmann[14] arrived at similar results to those in Ref. 15 by studying the dynamical susceptibility for localized spins within the framework of the Kondo lattice. Based on the proportionality of the linewidth with the inverse susceptibility, this investigation clearly shows the relevance of the ferromagnetic correlations, since a Curie-Weiss law with an antiferromagnetic Weiss temperature (Kondo effect) would produce a broad, and hence not observable, ESR line, while ferromagnetic correlations without long-range order enhance the susceptibility and hence can produce an observable resonance.

Several other approaches to explain the ESR in heavy-fermion systems have been proposed. Zvyagin *et al.*[17] considered a system with strong local anisotropic electron-electron interactions and showed that together with a hybridization between localized and itinerant electrons it may cause a g-shift of the ESR signal and a change in the linewidth. Huber,[18] on the other hand, studied the effects of anisotropy and the Yb-Yb interactions on the low-field ESR in $YbRh_2Si_2$ and $YbIr_2Si_2$ with main emphasis on the anisotropy of the g shift. Finally, for the anisotropic Kondo model with anisotropic Ruderman-Kittel-Kasuya-Yosida (RKKY) interaction, Kochelaev *et al.*[19] investigated the relaxation of a collective spin mode assuming that the Kondo coupling has the same anisotropy as the g factor.

The experimental interpretation[5] and some of the above theoretical studies[14,16,17,19,51] have the underlying assumption of a strong anisotropy leading to ferromagnetic correlations among the resonating spins. Recently, an ESR signal was observed at 60 GHz in the *cubic* compound CeB_6 in the temperature range from 1.8 to 3.8 K for the magnetic field parallel to the [110] direction.[20,21] The resonance[22] has a Dysonian-like line shape and a g factor of 1.59. The compound has a Kondo temperature of the order of 1 K and displays antiferro-quadrupolar order[23] where the resonance was observed. The crystalline field splitting of the Ce^{3+} ions in CeB_6 leads to a Γ_8 ground quartet,[24] which has simultaneously spin and quadrupolar content. The long-range order is driven by the quadrupolar degrees of freedom. There are several questions arising in the context of the observation of the ESR signal: (1) a Γ_8 quartet allows four transitions, why is only one observed? (2) The isotropy of the compound does not favor ferromagnetic correlations (the Curie-Weiss temperature arising from the Kondo effect has to be suppressed first), why is a resonance observed at all? (3) Can the resonance be understood within the single ion picture or is the signal necessarily due to itinerant electrons?

There was a report[25] on ESR in CeB_6 previous to those by Demishev *et al.*[20–22] where a resonance was seen in a temperature range up to 150 K. These results could not be reproduced by other groups.[22,26] There is a strong possibility that the ESR results are sample dependent.

In this paper, we present arguments that can explain why only one resonance is observed in CeB_6. The remainder of the article is organized as follows. In Sec. II, we lay the ground work by analyzing the transitions for a single Ce^{3+} ion with Γ_8 ground quartet for the magnetic field rotating in the $(1,-1,0)$ plane. This leads to four resonances for every angle of the magnetic field with the crystal axis. In Sec. III, we consider a single Ce^{3+} ion embedded in a lattice with antiferro-quadrupolar (AFQ) order. The long-range order with two sublattices reduces the four resonances to two signals, one for each sublattice. These results are extended to the full lattice in Sec. IV, where the $4f$ electrons are itinerant.[15,16] This reduces the two resonances to one resonance with g factor equal to the half sum of the g factors of the two sublattices. This allows us to conclude that the single-site picture cannot explain ESR in CeB_6. In Sec. V, we show that ferromagnetic spin correlations are generated via the quadrupolar correlations. These correlations explain the phase boundary between the AFQ and Kondo phases, the T and H dependence of the magnetization as well as the narrowing of the ESR linewidth. Hence it is unlikely that an ESR signal could be observed in a cubic Ce heavy-fermion compound with a Γ_7 ground doublet. Conclusions follow in Sec. VI. In Appendix A, the linewidth of the transitions discussed in Sec. II is addressed. The dynamical transversal susceptibility is expressed in terms of relaxation functions[27] for each of the transitions, yielding the Knight shift and the Korringa relaxation rate, as well as the proportionality relation of the relaxation time with the local static susceptibility. In Appendix B, we show that a single heavy-fermion band for the AFQ ordered lattice yields similar results as the two band Anderson lattice, namely, a single resonance with a g factor equal to the average of the g factors of the two sublattices.

II. SINGLE-SITE RESONANCES FOR A Ce ION WITH Γ_8 GROUND STATE

ESR of impurity rare-earth ions with Γ_8 ground quartets have been studied in several occasions, e.g., Dy^{3+} ions in the insulator[28] CaF_2 and the metal[29] Au, and Er^{3+} in the heavy-fermion low carrier compound[30] YbBiPt. Both Dy^{3+} and Er^{3+} ions have large total angular momenta of $J = 15/2$, and hence in cubic symmetry, two crystalline field parameters B_4 and B_6 are needed to characterize the splittings. The energy levels and the wave functions are then not universal, but depend on the parameter x related to B_4/B_6.[31]

This is different for Ce^{3+} ions, which have $J = 5/2$ and only require one crystalline field parameter, B_4. In a matrix with eightfold coordination, a Γ_8 ground quartet is expected with wave functions that can be expressed in terms of the J_z eigenstates:[31]

$$\begin{aligned} |+\uparrow\rangle &= \sqrt{\frac{5}{6}}\left|+\frac{5}{2}\right\rangle + \sqrt{\frac{1}{6}}\left|-\frac{3}{2}\right\rangle, \\ |+\downarrow\rangle &= \sqrt{\frac{5}{6}}\left|-\frac{5}{2}\right\rangle + \sqrt{\frac{1}{6}}\left|+\frac{3}{2}\right\rangle, \\ |-\uparrow\rangle &= \left|+\frac{1}{2}\right\rangle, \quad |-\downarrow\rangle = \left|-\frac{1}{2}\right\rangle. \end{aligned} \tag{1}$$

Here, $\uparrow$ and $\downarrow$ refer to the spin σ and $+$ and $-$ to the quadrupolar degrees of freedom.

The magnetization vector is given by $\vec{M} = \mu_B(\vec{L} + 2\vec{S})$ and the nonvanishing matrix elements of $\vec{M}$ are[32]

$$\begin{aligned} \langle +\sigma|M_z|+\sigma\rangle &= \tfrac{11}{7}\sigma\mu_B, \\ \langle -\sigma|M_z|-\sigma\rangle &= \tfrac{3}{7}\sigma\mu_B, \\ \langle -\downarrow|M_+|+\uparrow\rangle &= \langle +\downarrow|M_+|-\uparrow\rangle = \tfrac{4}{7}\sqrt{3}\mu_B, \\ \langle +\uparrow|M_+|+\downarrow\rangle &= \tfrac{10}{7}\mu_B, \\ \langle -\uparrow|M_+|-\downarrow\rangle &= \tfrac{18}{7}\mu_B, \end{aligned} \tag{2}$$

where σ takes values ± 1 and $M_\pm = M_x \pm iM_y$. For a magnetic field H parallel to the crystal [0, 0,1] direction (z axis), there are then four possible transitions:

$$\begin{aligned} |+\uparrow\rangle &\to |-\downarrow\rangle, \quad \Delta E = 2\mu_B H, \quad w = \tfrac{12}{49}, \\ |-\uparrow\rangle &\to |+\downarrow\rangle, \quad \Delta E = 2\mu_B H, \quad w = \tfrac{12}{49}, \\ |+\uparrow\rangle &\to |+\downarrow\rangle, \quad \Delta E = \tfrac{22}{7}\mu_B H, \quad w = \tfrac{25}{49}, \\ |-\uparrow\rangle &\to |-\downarrow\rangle, \quad \Delta E = \tfrac{6}{7}\mu_B H, \quad w = \tfrac{81}{49}, \end{aligned} \tag{3}$$

where ΔE is the corresponding transition energy and w the spectral weight (in arbitrary units) evaluated as the square of the matrix element of M_x. There are two more transition ($|+\uparrow\rangle \to |-\uparrow\rangle$ and $|-\downarrow\rangle \to |+\downarrow\rangle$), which for this direction of the magnetic field have zero spectral weight.

In ESR experiments, it is customary to rotate the magnetic field in the $(1,-1,0)$ plane. The magnetic field can then be parametrized as $\vec{H} = H(\sin\theta, \sin\theta, \sqrt{2}\cos\theta)/\sqrt{2}$, so that for $\theta = 0$ the field is along the [0,0,1] axis, if $\theta = \pi/2$ $\vec{H} \parallel$ [1,1,0], and for $\theta = \arctan(\sqrt{2}) = 54.7^o$ the magnetic field points into the [1,1,1] direction. The Zeeman Hamiltonian

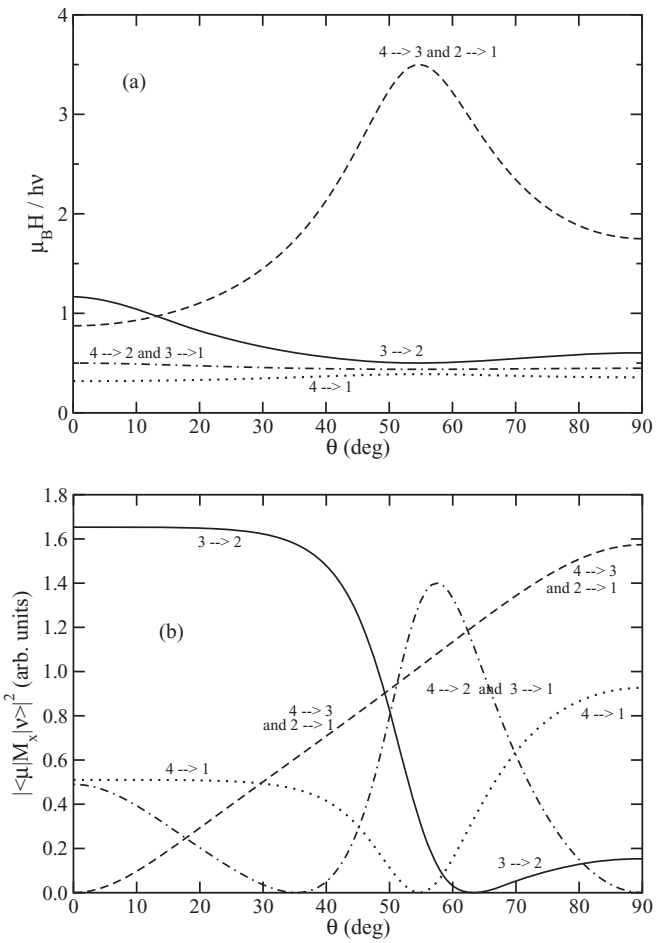

FIG. 1. (a) Transition fields normalized to the microwave energy $h\nu$ and (b) transition probabilities for a noninteracting Ce^{3+} in a Γ_8 quartet with Zeeman splitting for a magnetic field rotating in the $(1,-1,0)$ plane (angle θ). The four eigenstates are labeled with decreasing energy. States 1 with 4 and 2 with 3 form two spin Kramers doublets. There are no level crossings as a function of θ.

takes the form

$$\mathcal{H}_Z = -\vec{M}\cdot\vec{H} = -\tilde{M}_z H = -H\left(\frac{M_x + M_y}{\sqrt{2}}\sin\theta + M_z\cos\theta\right), \quad (4)$$

where M_x, M_y and M_z are 4×4 matrices defined by Eq. (2). Here, $\tilde{M}_z$ is the magnetization operator along the direction of the field. The Zeeman Hamiltonian is easily diagonalized numerically and the six transitions discussed in Eq. (3) now depend on the angle θ. The resonance fields $\mu_B H_r$ in units of $h\nu$ (where ν is the microwave frequency) are displayed in Fig. 1(a). We choose $\tilde{M}_x$ pointing into the $[1,-1,0]$ direction, which is always perpendicular to the direction of $\tilde{M}_z$. In terms of M_x and M_y for $\theta = 0$, we have that $\tilde{M}_x = (M_x - M_y)/\sqrt{2}$. The relative intensities of the transitions can now be calculated using the eigenstates of $\tilde{M}_z$ and are shown in Fig. 1(b). In Fig. 1, the eigenstates of $\tilde{M}_z$ are labeled in decreasing order of their energy. The four states correspond to two Kramers spin doublets, namely, states (1,4) and (2,3), the doublet (1,4) having the larger effective g factor. There are no level crossings as a function of θ. Note that the transitions $|4\rangle \to |3\rangle$ and $|2\rangle \to |1\rangle$ have the same resonance field and hence their transition probabilities have been added. Similarly for the transitions $|4\rangle \to |2\rangle$ and $|3\rangle \to |1\rangle$, which also have the same resonance fields.

In Eq. (1), we defined the four Γ_8 wave functions in terms of two indices, the spin σ ($\uparrow$ and $\downarrow$) and $+/-$ labeling the Kramers doublets. The latter represents the quadrupolar degrees of freedom of the quartet,[32] which are conveniently parametrized using a pseudospin description.[33,34] The spin and pseudospin operators are $1/2$ times Pauli matrices, denoted $\vec{\sigma}$ and $\vec{\tau}$, respectively, such that[32]

$$\begin{aligned} &\sigma_+|\pm\downarrow\rangle = |\pm\uparrow\rangle, \quad \sigma_-|\pm\uparrow\rangle = |\pm\downarrow\rangle, \\ &\sigma_z|\pm\sigma\rangle = \tfrac{1}{2}\sigma|\pm\sigma\rangle, \quad \tau_z|\pm\sigma\rangle = \pm\tfrac{1}{2}|\pm\sigma\rangle, \\ &\tau_+|-\sigma\rangle = |+\sigma\rangle, \quad \tau_-|+\sigma\rangle = |-\sigma\rangle. \end{aligned} \quad (5)$$

Using the above relations, the magnetic moment operator for the Γ_8 states can be written as[32]

$$M_\alpha = 2\mu_B\left(1 + \tfrac{8}{7}T_\alpha\right)\sigma_\alpha, \quad \alpha = x,y,z, \quad (6)$$

where

$$T_z = \tau_z, \quad T_x = -\frac{1}{2}\tau_z + \frac{\sqrt{3}}{2}\tau_x, \quad T_y = -\frac{1}{2}\tau_z - \frac{\sqrt{3}}{2}\tau_x. \quad (7)$$

Note that $\vec{M}$ does not depend on τ_y and the Zeeman Hamiltonian is still given by $\mathcal{H}_Z = -\vec{M}\cdot\vec{H}$.[32]

So far, we have discussed only the positions of the possible resonances. Their linewidth arises from the interaction with the electron gas. The formalism leading to the Lorentzian form of the transversal dynamical susceptibility[27] is sketched in Appendix A. This formalism leads to the proportionality of the relaxation time to the static susceptibility, i.e., the Korringa law for higher temperatures and the $1/T_{\rm rel} \approx T_K$ at low T. In the following section, we show that the long-range antiferro-quadrupolar order reduces the four single ion resonances to two.

III. SINGLE-SITE RESONANCES WITH ANTIFERRO-QUADRUPOLAR ORDER

When the temperature is lowered, CeB_6 undergoes a phase transition from the paramagnetic disordered phase into an antiferro-quadrupolar-ordered phase with $\vec{Q}$-vector along the $(1,1,1)$ directions.[23] The transition boundary is field dependent and T_c increases with magnetic field from 3.25 K at zero field to about 5.5 K at 4 T to 8.5 K at 15 T and almost 10 K at 30 T.[35]

The quadrupolar degrees of freedom are described by the Pauli matrices τ defined by Eq. (5).[32] Long-range order implies that the τ matrices are replaced by their eigenvalues. It is not known which combination of quadrupolar degrees of freedom provides the quadrupolar order at each site, i.e., the order does not necessarily form along τ_z. The magnetization operators (6) only depend on τ_x and τ_z, but not on τ_y. To define a general direction of the orbital order, it is then natural to rotate the τ matrices in the x-z plane, i.e.,

$$\begin{aligned} \tilde{\tau}_x &= \cos(\varphi)\tau_x - \sin(\varphi)\tau_z, \\ \tilde{\tau}_z &= \sin(\varphi)\tau_x + \cos(\varphi)\tau_z. \end{aligned} \quad (8)$$

Without loss of generality, we can now choose the quadrupolar order along $\tilde{\tau}_z$. We will consider two orientations of the magnetic field with the crystallographic axis. The simplest case corresponds to the magnetic field parallel to the crystal z axis. In the experimental situation,[20–22] the magnetic field points in the (1,1,0) direction.

A. $\vec{H} = H(0,0,1)$

The z component of the magnetization is given by Eq. (6). Inverting Eq. (8) and inserting into Eq. (6), we obtain

$$M_z = 2\mu_B\{1 + (8/7)[\cos(\varphi)\tilde{\tau}_z - \sin(\varphi)\tilde{\tau}_x]\}\sigma_z \,. \tag{9}$$

To introduce the antiferro-quadrupolar order, we replace $\tilde{\tau}_z$ by its eigenvalues, $\pm 1/2$. This way we assume the order is fully developed and along the direction of $\tilde{\tau}_z$. The quadrupolar fluctuations, represented by $\tilde{\tau}_x$, are taken into account by substituting $\tilde{\tau}_x$ by its expectation value, $\langle\tilde{\tau}_x\rangle = 0$. The g factors are then

$$g_\pm = 2 \pm (8/7)\cos(\varphi) \,. \tag{10}$$

For $\varphi = 0$, we recover $g_+ = 22/7$ and $g_- = 6/7$ in agreement with Eq. (3). There are then two simple resonances, one corresponding to each sublattice of the antiferro-quadrupolar order. Note that the originally four transitions (see Fig. 1) are reduced to two due to the antiferro-quadrupolar order.

Similarly, we can express M_x [see Eq. (6)] in terms of $\tilde{\tau}$ operators:

$$M_x = 2\mu_B\Bigg(1 + (8/7)\Bigg\{\left[-\frac{1}{2}\cos(\varphi) + \frac{\sqrt{3}}{2}\sin(\varphi)\right]\tilde{\tau}_z + \left[\frac{1}{2}\sin(\varphi) + \frac{\sqrt{3}}{2}\cos(\varphi)\right]\tilde{\tau}_x\Bigg\}\Bigg)\sigma_x \,. \tag{11}$$

With the same replacements as above, we have

$$M_x = \mu_B\left\{2 \pm (8/7)\left[-\frac{1}{2}\cos(\varphi) + \frac{\sqrt{3}}{2}\sin(\varphi)\right]\right\}\sigma_x \tag{12}$$

and the transition probabilities for the two sublattice sites are given by

$$|\langle\uparrow|M_x|\downarrow\rangle|^2 = \mu_B^2\left\{1 \pm (4/7)\left[-\frac{1}{2}\cos(\varphi) + \frac{\sqrt{3}}{2}\sin(\varphi)\right]\right\}^2 . \tag{13}$$

The resonance field and the spectral weights then depend on the angle φ determined by the linear combination of orbits in the antiferro-quadrupolar order. For $\varphi = 0$, we recover $w_+^2 = 25/49$ and $w_-^2 = 81/49$ in agreement with Eq. (3).

B. $\vec{H} = H(1,1,0)/\sqrt{2}$

This field direction is the one employed for the ESR measurements in CeB_6.[20–22] It is convenient to rotate the magnetization so that M_z^* is parallel to the magnetic field, i.e., we choose

$$M_z^* = (M_x + M_z)/\sqrt{2}, \quad M_x^* = (M_x - M_z)/\sqrt{2}, \quad M_y^* = M_y. \tag{14}$$

With the rotations of the τ matrices, Eq. (8), we obtain

$$M_z^* = \mu_B\sqrt{2}\Bigg(1 + (8/7)\Bigg\{\left[-\frac{1}{2}\cos(\varphi) + \frac{\sqrt{3}}{2}\sin(\varphi)\right]\tilde{\tau}_z + \left[\frac{1}{2}\sin(\varphi) + \frac{\sqrt{3}}{2}\cos(\varphi)\right]\tilde{\tau}_x\Bigg\}\Bigg)\sigma_x + \mu_B\sqrt{2}\{1 + (8/7)[\cos(\varphi)\tilde{\tau}_z - \sin(\varphi)\tilde{\tau}_x]\}\sigma_z \tag{15}$$

and imposing antiferro-quadrupolar order as in Sec. III A, we have

$$M_z^* = \mu_B\sqrt{2}\Bigg(\left\{1 \pm (4/7)\left[-\frac{1}{2}\cos(\varphi) + \frac{\sqrt{3}}{2}\sin(\varphi)\right]\right\}\sigma_x + [1 \pm (4/7)\cos(\varphi)]\,\sigma_z\Bigg) \,. \tag{16}$$

M_z^* is a 2×2 matrix in spin space that has to be diagonalized to obtain the effective g values

$$g_\pm = \sqrt{2}\{[1 \pm (4/7)\cos(\varphi)]^2 + [1 \mp (2/7)\cos(\varphi) \pm (2\sqrt{3}/7)\sin(\varphi)]^2\}^{1/2}. \tag{17}$$

Here, the $\pm$ refers to the sites of the two sublattices. The eigenstates are linear combinations of up-spin and down-spin states. Again, with antiferro-quadrupolar order there are only two resonances, rather than four (see Sec. II).

M_x^* can be obtained in a similar fashion:

$$\begin{aligned} M_x^* \;=\; & \mu_B\sqrt{2}\Bigg(1 + (8/7)\Bigg\{\left[-\frac{1}{2}\cos(\varphi) + \frac{\sqrt{3}}{2}\sin(\varphi)\right]\tilde{\tau}_z + \left[\frac{1}{2}\sin(\varphi) + \frac{\sqrt{3}}{2}\cos(\varphi)\right]\tilde{\tau}_x\Bigg\}\Bigg)\sigma_x \\ & -\mu_B\sqrt{2}\{1 + (8/7)[\cos(\varphi)\tilde{\tau}_z - \sin(\varphi)\tilde{\tau}_x]\}\sigma_z \\ \Longrightarrow\; & \mu_B\sqrt{2}\Bigg\{1 \pm (4/7)\left[-\frac{1}{2}\cos(\varphi) + \frac{\sqrt{3}}{2}\sin(\varphi)\right]\sigma_x - [1 \pm (4/7)\cos(\varphi)]\sigma_z\Bigg\}, \end{aligned} \tag{18}$$

and the spectral weight of the transition is given by the off-diagonal matrix elements of M_x^* within the eigenstates of M_z^*.

The g factors and the spectral weights for the two transitions are shown in Fig. 2 as a function of the quadrupolar mixing angle φ. If φ is continued into the interval π to 2π, the "+" solution goes over into the "−" solution and vice versa. So far, we considered full orbital order, which suppresses quadrupolar fluctuations. In principle, it is possible to introduce partial antiferro-quadrupolar order and quadrupolar fluctuations. The partial order shifts the g factors slightly and the fluctuations prevent g_+ and g_- from crossing, since the fluctuations act as a hybridization between the two resonances. The fluctuations also reinstate the two resonances suppressed by the full orbital order, but with a weak spectral weight proportional to the square of the fluctuations.

The main problem with the present formulation is that two resonances arise, one corresponding to sites of each sublattice. However, the system is not inhomogeneous and only one

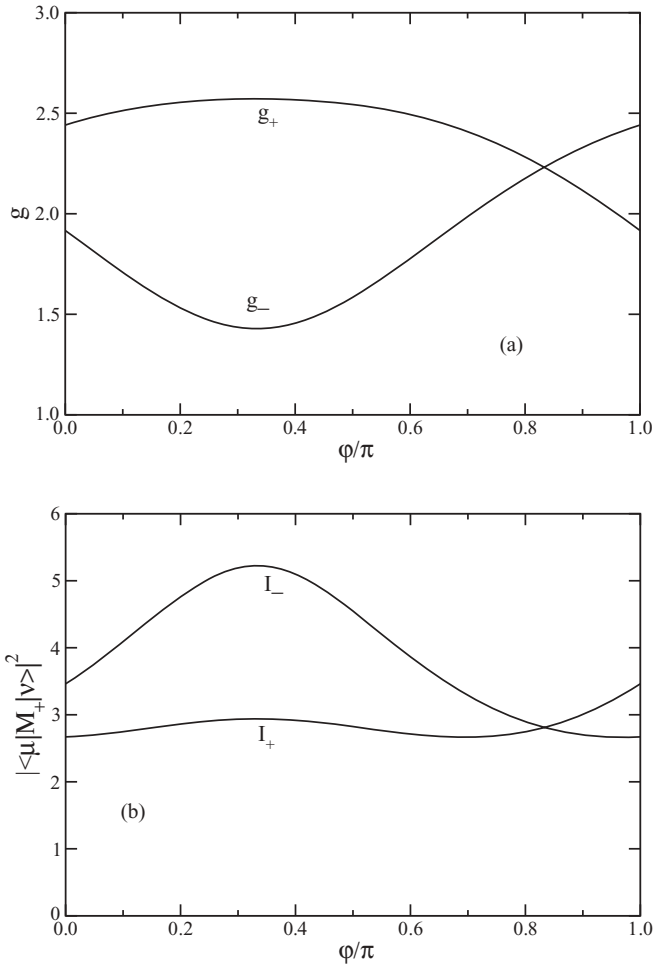

FIG. 2. (a) Effective g factors and (b) transition probabilities for a noninteracting Ce^{3+} in a Γ_8 quartet with Zeeman splitting for a magnetic field along the [1,1,0] direction for antiferro-quadrupolar order. φ is the hybridization angle for the quadrupolar degrees of freedom (see text).

resonance is observed. To correct for this fact, it is necessary to introduce coherence in the lattice, which is then not just a collection of independent sites.

IV. COHERENCE IN THE KONDO LATTICE

So far, we considered single-ion resonances and reduced the four transitions for the Ce^{3+} Γ_8 quartet to two resonances by imposing antiferro-quadrupolar order. These resonances correspond to a single resonance for the ions on each of the two sublattices. CeB_6 is a heavy-electron metal, so that the resonating electrons are not localized and are allowed to travel through the crystal. These itinerant electrons form a coherent state at low temperatures. This coherence reduces the two resonances discussed in Sec. III to a single resonance.

We consider two hybridized bands, a conduction and a localized electron band, and two interpenetrating sublattices, labeled with 1 and 2, respectively. The excluded double occupancy of the localized sites can be taken into account via slave bosons in the mean-field approximation, i.e., by replacing the hybridization V by a much smaller effective one $\tilde{V}$.[36,37] The hopping between sites of the conduction states conserves the spin component and the Hamiltonian can be written as the sum of one for up-spins and one for down spins. As a short-hand notation, we will suppress the spin index and write

$$\mathcal{H}_0 = \sum_{\vec{k}\alpha} \epsilon_{\vec{k}\alpha} c^\dagger_{\vec{k}\alpha} c_{\vec{k}\alpha} + \sum_j (\epsilon_1 d^\dagger_{1j} d_{1j} + \epsilon_2 d^\dagger_{2j} d_{2j}),$$
$$\mathcal{H}_V = \tilde{V} \sum_{\vec{k}\alpha j} (c^\dagger_{\vec{k}\alpha} d_{1j} e^{-i\vec{k}\vec{R}_j} + c^\dagger_{\vec{k}\alpha} d_{2j} e^{-i\vec{k}(\vec{R}_j+\vec{a})} + \text{H.c.}), \tag{19}$$

where $\vec{R}_j$ labels the sites of the sublattice 1 and $\vec{R}_j + \vec{a}$ the sites of the sublattice 2. There are then two Ce^{3+} ions per unit cell and $\alpha = a,b$ labels the two conduction bands in the reduced Brillouin zone. Fourier-transforming the site index j, the Hamiltonian has the form $\mathcal{H} = \sum_{\vec{k}} \mathcal{H}_{\vec{k}}$, where $\mathcal{H}_{\vec{k}}$ can be cast into the form of a 4×4 matrix. The diagonal part of the matrix contains the four one-particle energies and the off-diagonal entries are either $\tilde{V}$ or 0. The diagonalization of the matrix yields four bands separated by gaps. This picture is related to the Anderson lattice considered by Abrahams and Wölfle[15] with two main differences consisting in the slave-boson mean-field and the two sublattices with different on-site energies. The former simplifies the calculation, while the latter is specific to the CeB_6 problem.

For CeB_6, two electrons per Ce atom have to be placed into these bands, i.e., four into the reduced zone scheme. Including the spin index, there are two electrons per spin component. In zero magnetic field, $\epsilon_1 = \epsilon_2 = \epsilon$, i.e., the two quadrupolar states have the same energy (note that $\epsilon_1 \neq \epsilon_2$ implies a charge density wave), and we can assume that the Fermi level lies in the lower of the conduction bands. This way we can neglect the upper conduction band and reduce the dimension of the matrix to 3×3. Dropping the subindex α, the secular equation becomes

$$(\lambda - \epsilon_{\vec{k}})(\lambda - \epsilon_1)(\lambda - \epsilon_2) + \tilde{V}^2(2\lambda - \epsilon_1 - \epsilon_2) = 0\,. \tag{20}$$

For zero magnetic field, the roots of this cubic polynomial are

$$\lambda^*_0 = \epsilon \;\;,\;\; \lambda^*_\pm = \frac{\epsilon_{\vec{k}} + \epsilon}{2} \pm \frac{1}{2}\sqrt{(\epsilon_{\vec{k}} - \epsilon)^2 + 8\tilde{V}^2}\,, \tag{21}$$

i.e., there is one flat band, λ^*_0, and two dispersive bands, $\lambda^*_\pm$. The dispersive bands are essentially the standard hybridized bands of the Anderson lattice, which now has the dispersionless level in the center of the gap. A similar model has been proposed for $Ce_3Au_3Sb_4$,[38] which is a narrow-gap semiconductor with a very large density of localized states in the gap.

To discuss the general case, i.e., in a nonzero magnetic field, we introduce

$$\epsilon = (\epsilon_1 + \epsilon_2)/2 \;\;,\;\; \delta = (\epsilon_1 - \epsilon_2)/2\,, \tag{22}$$

or $\epsilon_1 = \epsilon + \delta$ and $\epsilon_1 = \epsilon - \delta$ and insert them into the secular equation,

$$\lambda^3 - \lambda^2(\epsilon_{\vec{k}} + 2\epsilon) + \lambda(2\epsilon_{\vec{k}}\epsilon + \epsilon^2 - \delta^2 - 2\tilde{V}^2)$$
$$-\epsilon_{\vec{k}}\epsilon^2 + \epsilon_{\vec{k}}\delta^2 + 2\tilde{V}^2\epsilon = 0\,. \tag{23}$$

For $\delta = 0$, the equation reduces to the one discussed before. δ represents the Zeeman splitting and is proportional to the magnetic field. It is useful to explicitly include the shift due to the Zeeman effect for the conduction electrons, by writing

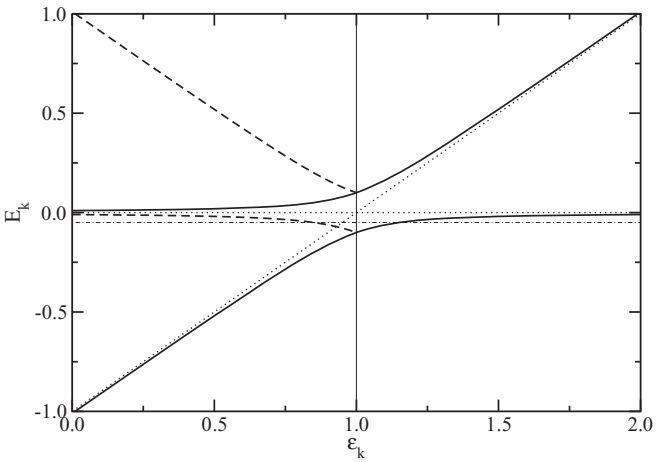

FIG. 3. Schematic hybridized bands: the dotted lines are the unhybridized dispersions for the conduction and localized states for the full Brillouin zone, the full curves are the hybridized bands showing a hybridization gap also for the full Brillouin zone, the dashed curves represent the folding of the hybridized bands into the reduced Brillouin zone, and the horizontal dash-dotted line displays the possible position of the Fermi level.

$\epsilon_{\vec{k}} \to \epsilon_{\vec{k}} + \epsilon_e$. To obtain the effective g factor, we are allowed to neglect all terms of order H^2.

Introducing $\lambda = \lambda^* + \delta\lambda$, we have

$$(\lambda^*)^3 - (\lambda^*)^2(\epsilon_{\vec{k}} + 2\epsilon) + \lambda^*(2\epsilon_{\vec{k}}\epsilon + \epsilon^2 - 2\tilde{V}^2)\epsilon - \epsilon_{\vec{k}}\epsilon^2 + 2\tilde{V}^2 + \delta\lambda[3(\lambda^*)^2 - 2\lambda^*(\epsilon_{\vec{k}} + 2\epsilon) + 2\epsilon_{\vec{k}}\epsilon + \epsilon^2 - \tilde{V}^2] - (\lambda^* - \epsilon)^2\epsilon_e = 0. \quad (24)$$

For $\delta\lambda = \epsilon_e = 0$, we recover the roots in Eq. (21); there is then the following relation between $\delta\lambda$ and ϵ_e:

$$\delta\lambda = \epsilon_e \frac{(\lambda^* - \epsilon)^2}{3(\lambda^*)^2 - 2\lambda^*(\epsilon_{\vec{k}} + 2\epsilon) + 2\epsilon_{\vec{k}}\epsilon + \epsilon^2 - \tilde{V}^2}, \quad (25)$$

which can be used to determine the effective g shift.

The simplest situation is when the Fermi level lies in the λ_0^* level. In this case, $\delta\lambda = 0$ and hence there is a single resonance with

$$g_{\rm eff} = (g_1 + g_2)/2\,, \quad (26)$$

where g_1 and g_2 are the g factors of the two sublattices as discussed in Sec. III. A more realistic assumption is that the Fermi level lies in one of the dispersive bands, but close to the hybridization gap. A simplified band picture is schematically shown in Fig. 3 for the full and reduced Brillouin zones for $\epsilon_1 = \epsilon_2$. A possible position for the Fermi level is shown as the horizontal dash-dotted line.

To evaluate the right-hand side of Eq. (25) in the general case, it is sufficient to neglect δ and to work in the full Brillouin zone. The hybridized band dispersions are

$$\lambda = \frac{\epsilon + \epsilon_{\vec{k}}}{2} \pm \frac{1}{2}\sqrt{(\epsilon - \epsilon_{\vec{k}})^2 + 4\tilde{V}^2}\,. \quad (27)$$

We consider the lower band and expand for small variations of ϵ and $\epsilon_{\vec{k}}$ due to the Zeeman shift and obtain

$$g_{\rm eff} = \frac{1}{2}\left(\frac{g_1 + g_2}{2} + g_e\right) - \frac{1}{2}\frac{\epsilon - \epsilon_{\vec{k}}}{\sqrt{(\epsilon - \epsilon_{\vec{k}})^2 + 4\tilde{V}^2}} \times \left(\frac{g_1 + g_2}{2} - g_e\right) = \frac{g_1 + g_2}{2} + {\rm corr}\,, \quad (28)$$

where corr is a correction term given by

$${\rm corr} = -\frac{1}{2}\left(\frac{g_1 + g_2}{2} - g_e\right)\left[1 - \frac{\epsilon - \epsilon_{\vec{k}}}{\sqrt{(\epsilon - \epsilon_{\vec{k}})^2 + 4\tilde{V}^2}}\right]. \quad (29)$$

For heavy fermions, the Fermi level intersects the lower band were $\epsilon - \epsilon_{\vec{k}} \gg 2V$, so that there is almost a complete cancellation of the two terms in the second bracket. Neglecting the corr term (there are uncertainties in the Knight shift of the resonance as well), we obtain *one resonance* with a g factor given by expression (26), i.e., the average g factor of the two sublattices for all cases. Note also that since the two sublattices have different g values, a uniform magnetic field induces a spin-density wave commensurate with the lattice of amplitude proportional to H. In Appendix B, we show that similar results are obtained for a single-band model of the t-J type.

V. MAGNETIC CORRELATIONS

Usually, in a heavy-fermion compound the rare-earth spins are antiferromagnetically correlated, even if the system does not undergo a phase transition to long-range order. The correlations have short-range character and the susceptibility follows a Curie-Weiss law with antiferromagnetic Weiss-temperature θ, $\chi_0 = C/(T + \theta)$, where θ is of the order of T_K. The relaxation rate is inversely proportional to χ_0 [see Eq. (A11)] and roughly follows a Korringa law, with a residual $T = 0$ linewidth proportional to θ. Hence the resonance can only be observed if θ is very small, i.e., of the order of 100 mK or less for X-band microwaves.[39] This would require an extremely narrow heavy fermion band or fermions with an effective mass of $10^5 m_e$, where m_e is the free electron mass. The T dependence in this case would be linear in T, i.e., a Korringa law.

If, on the other hand, the rare-earth spins are ferromagnetically correlated, the static susceptibility is given by $\chi_0 = C/(T - T_C)$ for $T > T_C$, where $T_C > 0$ is the Curie temperature. As $T \to T_C$, the susceptibility diverges and hence, according to expression (A11), the ESR linewidth becomes very narrow. This result has to be regarded with some caution, because we have neglected the relaxation through collective excitations, i.e., magnons. The ESR-signal found in single crystals of $YbRh_2Si_2$,[3] and other compounds[4–7] was attributed to the ferromagnetic correlations among the rare-earth spins and the strong magnetic anisotropy.[5] CeB_6 is an exception to this picture, since it is a cubic compound (very small magnetic anisotropy) and the ESR signal was observed in the antiferro-quadrupolar ordered phase. Below we present arguments on how ferromagnetic spin correlations can arise in CeB_6.

Consider the wave function for two electrons on neighboring sites. Each state consists of a coordinate wave function, an orbital (quadrupolar) wave function and a spin wave function. For the noninteracting system, the two-particle wave function then factors into a product of two-particle wave functions:

$$\Psi \sim \psi_{\rm coor}(\vec{r}_1,\vec{r}_2)\psi_{\rm orb}(m_1,m_2)\psi_{\rm spin}(\sigma_1,\sigma_2). \qquad (30)$$

The total wave function Ψ should be antisymmetric under the interchange of the indices 1 and 2. This implies that either one of the three factors in Eq. (30) is antisymmetric (and the other two symmetric) or all three factors have to be antisymmetric.

The wave function $\psi_{\rm coor}$ is the product of single site wave functions, $\varphi(\vec{r}_1)\varphi(\vec{r}_2)$, where both electrons are in the same state. This wave function is then necessarily symmetric. Hence out of $\psi_{\rm orb}(m_1,m_2)$ and $\psi_{\rm spin}(\sigma_1,\sigma_2)$ one has to be antisymmetric and the other one symmetric. We now assume that the effective two-particle interaction Hamiltonian is of the form $\mathcal{H}_{\rm int} = a\vec{\tau}_1 \cdot \vec{\tau}_2$, where a is the quadrupolar exchange. To be able to generate antiferro-quadrupolar order, necessarily a has to be positive. Hence $\psi_{\rm orb}(m_1,m_2)$ represents a singlet and has odd parity. Consequently, the spin wave function has to be a triplet (even parity). The spins are then ferromagnetically correlated.

The singlet state of the orbital degrees of freedom cannot be satisfied simultaneously between all the neighboring sites and generates a resonant valence bond lattice for the quadrupolar wave function. A magnetic field helps to align the spins and hence to enforce the antiferro correlations between the orbits. This could be the explanation of why the T_c of the phase boundary between the para-quadrupolar-disordered (Kondo) phase and the antiferro-quadrupolar phase increases with magnetic field. The magnetic field stabilizes the orbital order.

Some of the ferromagnetic correlations are expected to survive in the ordered phase and enhance the magnetic susceptibility, reducing the Weiss temperature and perhaps even changing its sign. At higher T, the Weiss θ is antiferromagnetic or Kondo-like, while when the phase boundary is approached θ becomes ferromagnetic[22] (see also Fig. 1 of Ref. 25). As seen in Eq. (A11), the relaxation rate is inversely proportional to the static transversal susceptibility, so that an enhanced χ_0^T reduces the linewidth and the resonance becomes observable. A similar conclusion, although with different arguments, has been presented in Ref. 22.

Quadrupolar degrees of freedom play a fundamental role in Ce^{3+} and Nd^{3+} ions with Γ_8 ground state.[40] They manifest themselves in first place through interactions among the sites. There is, however, no consensus about the origin of the interactions. Kubo and Kuramoto[41] successfully described the excitation spectrum of NdB_6 using nearest-neighbor intersite exchange and quadrupolar interactions. A different approach emphasizing crystalline fields was proposed by Uimin and Brenig.[42] For CeB_6, on the other hand, quadrupolar interactions between sites,[32] the RKKY interaction arising from the Coqblin-Schrieffer model,[43,44] and a detailed group theoretical study[45] have been presented.

VI. CONCLUSIONS

Generally, in heavy-fermion systems, an ESR signal cannot be observed because of antiferromagnetic correlations that broaden the line. At low temperatures, the linewidth is of the order of the Weiss temperature or T_K, and only with microwave frequencies of a few 100 GHz a signal could be detected. There are exceptions to this rule in magnetically very anisotropic compound with ferromagnetic correlations, e.g., $YbRh_2Si_2$,[3] $YbIr_2Si_2$,[4] CeRuPO,[7] YbRh,[5] and $YbCo_2Zn_{20}$.[6] The ferromagnetic correlations dramatically reduce the linewidth[5,14–16] so that a resonance can be seen with standard X- and Q-band frequencies.

CeB_6 constitutes an exception to the exceptions, since a resonance was observed in a cubic Kondo lattice in the antiferro-quadrupolar-ordered phase. ESR in this compound requires a separate explanation. The crystalline field ground state of each Ce ion is a Γ_8 quartet, which displays spin and quadrupolar degrees of freedom. From the antisymmetry of two-electron wave functions for neighboring sites, we conclude that in order to have antiferro-quadrupolar correlations necessarily the spins have to be ferromagnetically coupled. A magnetic field favors this state and the T_c of the phase boundary between the disordered Kondo phase and the phase with antiferro-quadrupolar order increases with H, in agreement with the experiment. Furthermore, the ferromagnetic correlations enhance the susceptibility (in agreement with experiment[22,25]) and hence reduce the linewidth of the resonance, which then becomes accessible to observation.

In the experimental papers,[3–5,9] the results for $YbRh_2Si_2$ have all been interpreted as if the resonance is due to localized f electrons. In other words, as for ESR on an impurity, if the microwave induces a spin flip at one site, the response of the system is measured at the same site. The response function in that case is the local dynamical susceptibility. The global dynamical susceptibility, on the other hand, is the Fourier-transform over the site pairs, $S(\mathbf{q},\omega)$, and ESR response corresponds to the $\mathbf{q} \to 0$ limit.[15] This appears to be the natural approach for extended conducting states.[16] However, since more than 60% of the Yb ions participate in the resonance,[13] it is hard to distinguish between the two approaches.[14]

Four resonances are expected from a single Ce^{3+} site with a Γ_8 ground quartet. Their resonance fields and spectral weights have been discussed in detail in Sec. II. The antiferro-quadrupolar order quenches three of these resonances at each site, leaving two resonances, one for each sublattice. Experimentally, however, only one resonance is observed. The ESR results for the system CeB_6 can therefore not be interpreted within the single site approach. The coherence in the global susceptibility reduces the two resonances to one with a g factor approximately given by the average of the g factors of the two sublattices. This average g factor depends on the angle φ of the quadrupolar order, and its value is of the order of 2 or slightly larger. The experimentally observed g value[20–22] is about 1.6, i.e., considerably smaller than the theoretical value. The Knight shift due to the exchange in the Coqblin-Schrieffer model yields a correction (of about 10% of g) in the right direction. However, even if we consider the contribution of the four conduction channels coupling to the Γ_8 multiplets, the Knight shift is probably not large enough to account for the difference. There is also the possibility that the quadrupolar order, the intersite interactions and the

coherence of the lattice change the Knight g shift into the correct direction.

Experimentally, the resonance has a dysonian line shape and the linewidth[22] is a Korringa law at low T ($1.8 \leqslant T \leqslant 3.0$ K). When T is extrapolated to zero, there is only a small residual linewidth left. This indicates that the antiferro-quadrupolar order and the ferromagnetic correlations between spins are effective in preventing the Kondo effect to develop in the ordered phase. At larger T ($3.0 \leqslant T \leqslant 3.8$ K) the linewidth is larger than the Korringa law. There are two possible explanations for this enhancement: (i) the modulation of the ligand field by lattice vibrations causes, by means of the spin-orbit coupling, a spin-lattice relaxation (Orbach relaxation process[46]), which depends exponentially on the thermal activation of the excited Γ_7 crystalline field state [the splitting between the Γ_8 and Γ_7 multiplets is 530 K (see Ref. 47)], and (ii) the relaxation increases because the phase boundary is approached and quadrupolar fluctuations consequently become larger and favor spin-lattice relaxation.

In summary, the reason why an ESR line is observed in CeB_6 is very different from that of the other compounds. CeB_6 is cubic and hence magnetically only weakly anisotropic. It requires a Γ_8 ground state with antiferro-quadrupolar correlations to enhance the spin susceptibility and reduce this way the linewidth. The single resonance observed in CeB_6 is evidence (in conjunction with the analysis in Ref. 16) that the ESR signal is a collective phenomenon involving all the sites of the lattice. Note also that in a cubic compound with Γ_7 ground doublet antiferromagnetic correlations are induced and hence an ESR signal is too broad to be observed with standard techniques. The Γ_8 ground state and the antiferro-quadrupolar order are essential ingredients for the observability of an ESR signal in a cubic environment.

ACKNOWLEDGMENTS

The support by the US Department of Energy under grant DE-FG02-98ER45707 is acknowledged. The author is thankful to S.B. Oseroff, C. Rettori, and G. Barberis for helpful comments.

APPENDIX A: RELAXATION FUNCTIONS

In this Appendix, we present a sketch of a calculation of the dynamical transversal susceptibility, the Knight shift and the relaxation rates of the four resonances discussed in Sec. II. We follow the procedure developed in Ref. 27 for a spin S. The dynamics described by this method is equivalent to Bloch's equations.[48] The present is an extension of Refs. 1,14, and 27 to many resonances due to the crystalline field splitting.

The Ce^{3+} site interacts with the conduction states via the Coqblin-Schrieffer exchange Hamiltonian, $\mathcal{H} = \mathcal{H}_0 + \mathcal{H}_{CS}$,

$$\begin{aligned} \mathcal{H}_0 &= \sum_{km} \epsilon_{km} c^\dagger_{km} c_{km} + \sum_m E_m, \\ \mathcal{H}_{CS} &= \frac{J}{N} \sum_{kk'mm'} \left[1 - \frac{1}{4} \delta_{mm'} \right] c^\dagger_{km} |m'\rangle\langle m| c_{k'm'}, \end{aligned} \tag{A1}$$

where $\mathcal{H}_0$ represents the kinetic energy of the conduction electrons (in principle, there are three elliptic bands centered about the X points in CeB_6) and the Zeeman splitting of the four Ce-Γ_8 states, which are labeled here with $m = 1, \ldots, 4$. The energies E_m are proportional to the field H and depend on the angle between the field and the crystallographic axis as discussed in Sec. II. The Ce site under consideration is the origin of the coordinate system and c_{km} refers to the conduction state with momentum $k = |\mathbf{k}|$ and partial wave m. $\mathcal{H}_{CS}$ has been defined so that its trace is zero. J is the exchange coupling and N the number of sites in the lattice.

The ESR response is determined by the transversal dynamical susceptibility corresponding to a transition. Without loss of generality, we can consider the transition between the states m_1 and m_2. Assuming that $E_{m_2} > E_{m_1}$, the operator inducing the transition is $A^\dagger_{m_1m_2} = |m_1\rangle\langle m_2|$ (for a two level system $A^\dagger$ corresponds to the raising operator S^+) and we can define the spin-current operator as

$$\begin{aligned} j^\dagger_{m_1m_2} = [|m_1\rangle\langle m_2|, \mathcal{H}_{CS}] = \frac{J}{N} \sum_{kk'm} (c^\dagger_{km} c_{k'm_2} |m_1\rangle\langle m| \\ - c^\dagger_{km_1} c_{k'm} |m\rangle\langle m_2|). \end{aligned} \tag{A2}$$

Taking the expectation value of the conduction states, we obtain

$$\begin{aligned} j^{\dagger\langle av\rangle}_{m_1m_2} &= \frac{J}{N} \sum_k (f(\epsilon_{km_2}) - f(\epsilon_{km_1})) |m_1\rangle\langle m_2| \\ &= -J\rho(E_{m_2} - E_{m_1}) |m_1\rangle\langle m_2|, \end{aligned} \tag{A3}$$

where ρ is the conduction density of states. This term renormalizes the Zeeman splitting of the Γ_8 states and corresponds to the Knight shift of the magnetic resonance. It is convenient to work with the Hartree-Fock factored variant of H_{CS}, i.e., we include the Knight shift into the energies E_m.

We define the correlation function for the transition as

$$\chi^T_{m_1m_2}(z) = -\mu_B^2 \langle\langle A^\dagger_{m_1m_2}; A_{m_1m_2} \rangle\rangle_z \,. \tag{A4}$$

For $S = 1/2$, this response function corresponds to the transversal susceptibility. Following Götze and Wölfle,[27] we write

$$\chi^T_{m_1m_2}(z) = \frac{N^T_{m_1m_2}(z) - \mu_B^2 \langle [A^\dagger_{m_1m_2}, A_{m_1m_2}] \rangle}{z - (E_{m_2} - E_{m_1}) + N^T_{m_1m_2}(z)/\chi^T_0} \,, \tag{A5}$$

which defines the function $N^T_{m_1m_2}(z)$ and $\chi^T_0 = \chi^T_{m_1m_2}(z = 0)$ is the static transversal response function. The important part of $N^T_{m_1m_2}(z)$ is its imaginary part at the resonance, i.e., for $z = E_{m_2} - E_{m_1}$, which divided by χ^T_0 yields the relaxation rate. The function $N^T_{m_1m_2}(z)$ is analytic in the complex upper and lower frequency half planes and falls off as $1/z$ for large z (see Ref. 27). To simplify, we will use the short-hand notation $\chi^T_{m_1m_2}(z) = \chi_{12}(z)$, $N^T_{m_1m_2}(z) = N_{12}(z)$, $E_{m_2} - E_{m_1} = h_{21}$, etc.

It is instructive to calculate the relaxation function $N_{12}(z)$ to second order in J. The imaginary part of the relaxation function $N_{12}(z)$ is given by the spin-current correlation function[27]

$$N''_{12}(\omega) = -\left(\mu_B^2/\omega\right) \left\langle\!\left\langle j^{(c)}_{12}; j^{(c)\dagger}_{12} \right\rangle\!\right\rangle''_\omega, \tag{A6}$$

where $j_{12}^{(c)} = j_{12} - j_{12}^{\langle av\rangle}$ is the Hartree-Fock corrected spin current operator. We obtain

$$N''_{12}(\omega) = \pi(J\rho\mu_B)^2\left[\frac{e^{-E_1/T}+e^{-E_2/T}}{Z} + 2\phi_{12}(\omega)\right] + \pi(J\rho\mu_B)^2[\phi_{13}(\omega)+\phi_{14}(\omega)+\phi_{32}(\omega)+\phi_{42}(\omega)], \tag{A7}$$

where $Z = \sum_{i=1}^{4} e^{-E_i/T}$ is the partition function of the quadruplet and

$$\phi_{ij}(\omega) = \frac{\omega - h_{ji}}{2\omega}\frac{e^{-E_i/T}-e^{-E_j/T}}{Z} \times\left[\coth\left(\frac{\omega-h_{ji}}{2T}\right)+\coth\left(\frac{h_{ji}}{2T}\right)\right]. \tag{A8}$$

The first bracket of Eq. (A7) is the contribution involving only the levels 1 and 2 and is similar to the one obtained in Ref. 27 for a spin 1/2 system. The second bracket represents the contributions involving the intermediate states 3 and 4. These terms do not appear for a spin 1/2 system. The static susceptibility χ_0^T for the states m_1 and m_2 is given by

$$\chi_0^T = \mu_B^2\frac{e^{-E_2/T}-e^{-E_1/T}}{h_{21}Z}. \tag{A9}$$

For small frequencies and in the high-temperature limit, i.e., for T larger than the Zeeman splittings, the functions $\phi_{ij}(\omega)$ approach the constant 1/4. From Eq. (A5) it is seen that the dynamical response function has a Lorentzian shape with a relaxation rate[27]

$$1/T_{\rm rel} = N''_{12}(\omega=0)/\chi_0^T = 2\pi(J\rho)^2 4T. \tag{A10}$$

This expression is essentially the well-known Korringa relaxation rate, i.e., the linewidth is proportional to the temperature. The difference with the standard relaxation rate for a spin 1/2 and the s-d Kondo Hamiltonian is a factor of eight; a factor of four can be attributed to the definition of the exchange coupling ($J_{sd} = 2J$) and a factor of two arises from the contributions to N''_{12} from the intermediate states 3 and 4.

The Korringa relaxation rate can also be obtained via Fermi's golden rule by calculating the spin transfer to the conduction electrons via exchange scattering. In this case, the factor T arises from the fraction of the Fermi sea that is available for scattering. The relaxation function method yields the same result, but the factor T comes from the susceptibility. The relaxation function method can be derived from Bloch's equations[48] or justified from the Mori-Zwanzig projector formalism.[49,50] The method has also been used by Huber in his treatment of electron paramagnetic resonance in exchange-coupled systems with unlike spins.[51]

The above calculation is the extension of the formalism of Ref. 27 for $S = 1/2$ to a more complex situation involving four states. It is interesting to point out that the T dependence of the relaxation rate arises from the static susceptibility. We obtain this way that[1]

$$T_{\rm rel} \propto \chi_0^T, \tag{A11}$$

as stated in Introduction.

The frequency dependence of N''_{12} at temperatures less than the Zeeman spitting can give rise to retardation effects.[27] At low frequencies, the relaxation is suppressed since the transition has to overcome the Zeeman splitting and the energy of the thermal bath is not sufficient for this. However, the experiments for CeB_6 were carried out $T > 1.8$ K and at 60 GHz, which translated to temperatures corresponds to 1.5 K, so that the temperature is always larger than the Zeeman splitting. Retardation effects then do not play a relevant role.

Perturbatively in J the Kondo effect introduces logarithmic divergencies as a function of T and B, which eventually give rise to the screening of the spin. The Kondo effect affects both, the relaxation function $N^T(z)$ and the static susceptibility χ_0^T. The relaxation function is enhanced by the Kondo effect [$N^T(0)$ reaches the Shiba[2] unitarity limit $N^T(0) = i(g\mu_B)^2 2/\pi$ for $S = 1/2$] and the static susceptibility decreases reaching a constant value, inversely proportional to T_K. Hence, the relaxation rate is considerably enhanced, rendering the resonance too broad to be observed (only if T_K is less than 100 mK an ESR resonance would be observable in X band[39]). In CeB_6, however, $T_K \sim 1$ K, so that for $T > 1.8$ K and due to the antiferro-quadrupolar order, the Kondo screening is not fully developed. For the temperature regime of interest, the susceptibility is a Curie-Weiss law with antiferromagnetic Weiss temperature $\theta \approx -2T_K$ and the linewidth is still too large to be observed with X-band or Q-band spectrometers.

When the Ce-ion under consideration is embedded into a magnetic lattice (antiferromagnetic or ferromagnetic), the mean field of the surroundings modifies the static susceptibility to a Curie-Weiss law with a $\theta_{\rm CW}$. In the paramagnetic phase, the proportionality of $T_{\rm rel} \approx \chi_0 \approx 1/(T-\theta)$ is then favorable for the observation of an ESR signal in the ferromagnetic case, but not in the antiferromagnetic situation.

The total intensity of the line is the integral over the resonance times the square of the matrix element of M_x (spectral weight), as discussed in Sec. II. In the absence of retardation effects, this yields $\pi|\langle 1|M_x|2\rangle|^2\chi_0^T$, i.e., the intensity of the line is proportional to the corresponding susceptibility. If the system has several transitions that are well separated, the spectrum is given by the sum of the corresponding dynamic response functions times their spectral weight. If two transitions have the same resonance field (as, e.g., $4 \to 2$ and $3 \to 1$ or $4 \to 3$ and $2 \to 1$ in Fig. 1), then the response functions are the same and have a spectral weight corresponding to the sum of the spectral weights. Finally, in the general case, when two or more resonance fields are similar, it is necessary to introduce a matrix response function and a corresponding relaxation matrix[52] with the transitions to be considered as entries. When the resonances are sufficiently separated, the matrix formalism reduces again to individual resonances.

In summary, in the present appendix, we have generalized the resonance formalism of Ref. 27 for a general spin S to a system with multiple possible resonances.

APPENDIX B: SINGLE-BAND MODEL

In Sec. IV, we studied a two-band model involving a flat band of localized states hybridized with a dispersive

conduction band and concluded that as a consequence of the lattice coherence the two sublattice resonances reduce to one with the g factor approximately given by the average of the g factors of the two sublattices. In this appendix, we show that a similar result is obtained within a single-band model (of the t-J family).

We consider one tight-binding band with two interpenetrating sublattices 1 and 2. The unit cell has two sites of one-electron energies ϵ_1 and ϵ_2, respectively. Correlations can be taken into account in mean field, reducing the hopping matrix element to a smaller effective one. As in Sec. IV, we suppress the spin index. In the reduced Brillouin zone, the one-electron Hamiltonian is then

$$\mathcal{H} = \sum_{\vec{k}} \left[\epsilon_1 c^\dagger_{\vec{k}1} c_{\vec{k}1} + \epsilon_2 c^\dagger_{\vec{k}2} c_{\vec{k}2} + \epsilon_{\vec{k}} \left(c^\dagger_{\vec{k}1} c_{\vec{k}2} + c^\dagger_{\vec{k}2} c_{\vec{k}1}\right)\right], \quad \text{(B1)}$$

where $\epsilon_{\vec{k}} = -2t \sum_i \cos(\vec{k} \cdot \vec{R}_i)$ with $\vec{R}_i$ being the vectors joining the nearest neighbor sites.

The Hamiltonian is easily diagonalized for each value of $\vec{k}$ and the eigenvalues are

$$\lambda = \frac{\epsilon_1 + \epsilon_2}{2} \pm \frac{1}{2}\sqrt{(\epsilon_1 - \epsilon_2)^2 + 4\epsilon^2_{\vec{k}}}\,. \quad \text{(B2)}$$

For antiferro-quadrupolar order and in zero field $\epsilon_1 = \epsilon_2$, so that with an applied magnetic field $(\epsilon_1 - \epsilon_2)^2 \sim H^2$ (which can be neglected for the purpose of a g-factor calculation), and the effective g factor is

$$g_{\rm eff} = \frac{g_1 + g_2}{2}\,, \quad \text{(B3)}$$

in agreement with the result in Sec. IV, Eq. (26).

[1] W. Götze and P. Schlottmann, Solid State Commun. **13**, 17 (1973); **13**, 861 (1973); J. Low Temp. Phys. **16**, 87 (1974).

[2] K. Yamada, Prog. Theor. Phys. **53**, 970 (1975); H. Shiba, *ibid.* **54**, 967 (1975).

[3] J. Sichelschmidt, V. A. Ivanshin, J. Ferstl, C. Geibel, and F. Steglich, Phys. Rev. Lett. **91**, 156401 (2003).

[4] J. Sichelschmidt, J. Wykhoff, H.-A. Krug von Nidda, I. I. Fazlishanov, Z. Hossain, C. Krellner, C. Geibel, and F. Steglich, J. Phys.: Condens. Matter **19**, 016211 (2007).

[5] C. Krellner, T. Förster, H. Jeevan, C. Geibel, and J. Sichelschmidt, Phys. Rev. Lett. **100**, 066401 (2008).

[6] V. A. Ivanshin, A. A. Sukhanov, D. A. Sokolov, M. C. Aronson, S. Jia, S. L. Bud'ko, and P. C. Canfield, J. Alloys Compd. **480**, 126 (2009).

[7] E. M. Bruning, C. Krellner, M. Baenitz, A. Jesche, F. Steglich, and C. Geibel, Phys. Rev. Lett. **101**, 117206 (2008).

[8] V. A. Ivan'shin, L. K. Aminov, I. N. Kurkin, J. Sichelschmidt, O. Stockert, J. Ferstl, and C. Geibel, Pis'ma Zh. Eksp. Teor. Fiz. **77**, 625 (2003) [JETP Lett. **77**, 526 (2003)].

[9] J. G. S. Duque, E. M. Bittar, C. Adriano, C. Giles, L. M. Holanda, R. Lora-Serrano, P. G. Pagliuso, C. Rettori, C. A. Pérez, R. W. Hu, C. Petrovic, S. Maquilon, Z. Fisk, D. L. Huber, and S. B. Oseroff, Phys. Rev. B **79**, 035122 (2009).

[10] U. Schaufuss, V. Kataev, A. A. Zvyagin, B. Büchner, J. Sichelschmidt, J. Wykhoff, C. Krellner, C. Geibel, and F. Steglich, Phys. Rev. Lett. **102**, 076405 (2009).

[11] G. Feher and A. F. Kip, Phys. Rev. **98**, 337 (1955); F. J. Dyson, *ibid.* **98**, 349 (1955); G. E. Pake and E. M. Purcell, *ibid.* **74**, 1184 (1948).

[12] C. Rettori, D. Davidov, R. Orbach, E. P. Chock, and B. Ricks, Phys. Rev. B **7**, 1 (1973); C. Rettori, D. Davidov, and H. M. Kim, *ibid.* **8**, 5335 (1973); C. Rettori, H. M. Kim, E. P. Chock, and D. Davidov, *ibid.* **10**, 1826 (1974).

[13] J. Sichelschmidt, J. Wykhoff, H.-A. Krug von Nidda, J. Ferstl, C. Geibel, and F. Steglich, J. Phys.: Condens. Matter **19**, 116204 (2007); J. Sichelschmidt, V. A. Ivan'shin, J. Ferstl, C. Geibel, and F. Steglich, J. Magn. Magn. Mater. **272**, 42 (2004); **276**, 42 (2004).

[14] P. Schlottmann, Phys. Rev. B **79**, 045104 (2009).

[15] E. Abrahams and P. Wölfle, Phys. Rev. B **78**, 104423 (2008).

[16] P. Wölfle and E. Abrahams, Phys. Rev. B **80**, 235112 (2009).

[17] A. A. Zvyagin, V. Kataev, and B. Büchner, Phys. Rev. B **80**, 024412 (2009).

[18] D. L. Huber, J. Phys.: Condens. Matter **21**, 322203 (2009).

[19] B. I. Kochelaev, S. I. Belov, A. M. Skvortsova, A. S. Kutuzov, J. Sichelschmidt, J. Wykhoff, C. Geibel, and F. Steglich, Eur. Phys. J. B **72**, 485 (2009).

[20] S. V. Demishev, A. V. Semeno, Yu.B. Paderno, N. Yu. Shitsevalova, and N. E. Sluchanko, Phys. Status Solidi B **242**, R27 (2005).

[21] S. V. Demishev, A. V. Semeno, A. V. Bogach, Yu.B. Paderno, N. Yu. Shitsevalova, and N. E. Sluchanko, J. Magn. Magn. Mater. **300**, e-534 (2006).

[22] S. V. Demishev, A. V. Semeno, A. V. Bogach, N. A. Samarin, T. V. Ishchenko, V. B. Filipov, N. Yu. Shitsevalova, and N. E. Sluchanko, Phys. Rev. B **80**, 245106 (2009).

[23] J. Effantin, J. Rossat-Mignod, P. Burlet, H. Bartholin, S. Kunii, and T. Kasuya, J. Magn. Magn. Mater. **47**, 145 (1985); **48**, 145 (1985).

[24] T. Fujita, M. Suzuki, T. Komatsubara, S. Kunii, T. Kasuya, and T. Ohtsuka, Solid State Commun. **35**, 569 (1980).

[25] C. Terzioglu, D. A. Browne, R. G. Goodrich, A. Hassan, and Z. Fisk, Phys. Rev. B **63**, 235110 (2001).

[26] S. B. Oseroff and C. Rettori (private communication).

[27] W. Götze and P. Wölfle, J. Low Temp. Phys. **5**, 575 (1971).

[28] R. W. Bierig and M. J. Weber, Phys. Rev. **132**, 164 (1963).

[29] D. Davidov, R. Orbach, C. Rettori, L. J. Tao, and E. P. Chock, Phys. Rev. Lett. **28**, 490 (1972).

[30] G. B. Martins, D. Rao, G. E. Barberis, C. Rettori, R. J. Duro, J. Sarrao, Z. Fisk, S. Oseroff, and J. D. Thompson, Phys. Rev. B **52**, 15062 (1995).

[31] K. R. Lea, M. J. M. Leask, and W. P. Wolf, J. Phys. Chem. Solids **23**, 1381 (1962).

[32] G. Uimin, Y. Kuramoto, and N. Fukushima, Solid State Commun. **97**, 595 (1996).

[33] K. I. Kugel and D. I. Khomskii, Sov. Phys. JETP **37**, 725 (1973).

[34] F. J. Ohkawa, J. Phys. Soc. Jpn. **52**, 3897 (1983).

[35] D. Hall, Z. Fisk, and R. G. Goodrich, Phys. Rev. B **62**, 84 (2000); R. G. Goodrich, D. P. Young, D. Hall, L. Balicas, Z. Fisk, N. Harrison, J. Betts, A. Migliori, F. M. Woodward, and J. W. Lynn, *ibid.* **69**, 054415 (2004).

[36] N. Read and D. M. Newns, J. Phys. C **16**, L1055 (1983).

[37] P. Coleman, Phys. Rev. B **29**, 3035 (1984).

[38]H.-O. Lee, Y.-J. Jo, L. Balicas, P. Schlottmann, C. L. Condron, V. A. Sidorov, P. Klavins, S. M. Kauzlarich, J. D. Thompson, and Z. Fisk, Phys. Rev. B **76**, 155204 (2007).
[39]Y. von Spalden, E. Tsang, K. Baberschke, and P. Schlottmann, Phys. Rev. B **28**, 24 (1983); **29**, 487(E) (1984).
[40]J. Stankiewicz, M. Evangelisti, Z. Fisk, P. Schlottmann, and L.P. Gor'kov, Phys. Rev. Lett. **108**, 257201 (2012).
[41]K. Kubo and Y. Kuramoto, J. Phys.: Condens. Matter **15**, S2251 (2003).
[42]G. Uimin and W. Brenig, Phys. Rev. B **61**, 60 (2000).
[43]F. J. Ohkawa, J. Phys. Soc. Jpn. **54**, 3909 (1985).
[44]P. Schlottmann, Phys. Rev. B **62**, 10067 (2000).
[45]R. Shiina, H. Shiba, and P. Thalmeier, J. Phys. Soc. Jpn. **66**, 1741 (1997).
[46]R. Orbach, Proc. R. Soc. London A **264**, 458 (1961).
[47]E. Zirngiebl, B. Hillebrands, S. Blumenröder, G. Güntherodt, M. Loewenhaupt, J. M. Carpenter, K. Winzer, and Z. Fisk, Phys. Rev. B **30**, 4052 (1984).
[48]F. Bloch, Phys. Rev. **70**, 460 (1946).
[49]H. Mori, Prog. Theor. Phys. (Kyoto) **34**, 399 (1965).
[50]R. Zwanzig, J. Chem. Phys. **33**, 1338 (1960).
[51]D. L. Huber, Phys. Rev. B **12**, 31 (1975); **13**, 291 (1976).
[52]W. Götze and P. Wölfle, J. Low Temp. Phys. **6**, 455 (1972).